

Exposure-Tolerant Imaging Solution for Cultural Heritage Monitoring

*Original*

Exposure-Tolerant Imaging Solution for Cultural Heritage Monitoring / Corbellini, Simone; Ferraris, Franco; Neri, Alessandra; Parvis, Marco; Angelini, EMMA PAOLA MARIA VIRGINIA; Grassini, Sabrina. - In: IEEE TRANSACTIONS ON INSTRUMENTATION AND MEASUREMENT. - ISSN 0018-9456. - STAMPA. - 60:5(2011), pp. 1691-1698. [10.1109/TIM.2010.2090191]

*Availability:*

This version is available at: 11583/2380897 since:

*Publisher:*

IEEE / Institute of Electrical and Electronics Engineers Incorporated:445 Hoes Lane:Piscataway, NJ 08854:

*Published*

DOI:10.1109/TIM.2010.2090191

*Terms of use:*

This article is made available under terms and conditions as specified in the corresponding bibliographic description in the repository

*Publisher copyright*

(Article begins on next page)

# Exposure tolerant imaging solution for cultural heritage monitoring

Simone Corbellini, Franco Ferraris, Alessandra Neri, Marco Parvis, *Fellow, IEEE*,

Emma Angelini, Sabrina Grassini

**Abstract**—This paper describes a simple and cheap solution specifically designed for monitoring the degradation of thin coatings employed for metal protection. The proposed solution employs a commercial photcamera and a frequency domain based approach, that is capable of highlighting the surface uniformity changes due to the initial corrosion. Even though the proposed solution is specifically designed to monitor the long-time performance of protective coatings employed for restoration of silver artifacts, it can be successfully used also for assessing the conservation state of other ancient metallic works of art. The proposed solution is made tolerant to exposure changes by using a procedure for sensor non-linearity identification and correction, does not require a precise lighting control and employs only free, open source software; so that its overall cost is very low, and can be used also by not specifically trained operators.

Cultural heritage, FFT, digital photography, imaging, corrosion

## I. INTRODUCTION

Heritage metallic works of art are subjected to degradation due to the presence of environmental humidity and pollution thus protective coatings are often used for their preservation. Such coatings have to be transparent and thin to avoid altering the artifact aesthetical appearance and must be easily removable to avoid a permanent artifact alteration. Unfortunately these requirements often turn out in coatings subjected to degradation, that must be periodically replaced. It is, therefore, important to have a system for easily monitoring the surface condition helping conservators to decide when an action is required. The coating protective effectiveness is usually assessed by means of electrochemical techniques, such as electrochemical impedance spectroscopy (EIS), while the degradation of metallic surfaces can be monitored by using analytical techniques and high resolution microscopies; these approaches allow scientists to identify the degradation mechanism, the entity and the rate of the corrosion process, but often require an artifact manipulation which can speed up the degradation and should, therefore, be avoided. A solution which appears quite attractive to avoid any manipulation is the use of a visual inspection based on digital imaging. Unfortunately, most image based approaches require a tight light control in order to obtain reproducible results and this may be difficult to obtain in a museum without impairing the object fruition.

S. Corbellini, F. Ferraris, A. Neri and M. Parvis are with the Dipartimento di Elettronica, E. Angelini and S. Grassini are with the Dipartimento di Scienza dei Materiali e Ingegneria Chimica, Politecnico di Torino, corso Duca degli Abruzzi, 24 - 10129 Torino (Italy); phone: +39 011 5644114, fax: +39 011 5644217, e-mail: marco.parvis@polito.it

In this paper an easy-to-use and cheap tool for works of art surface analysis, which is based on digital photography, a pre-processing to linearize the camera sensor response and a 2D-FFT (Fast Fourier Transform) image processing, is described with the final aim of proposing this approach for the in situ monitoring of the conservation state of metallic antiquities.

The complete image processing takes only a few seconds including the image transfer from camera to PC so that the proposed solution can be also used for routine checks of the antiquity conservation state

## II. THE PROPOSED FREQUENCY DOMAIN IMAGE PROCESSING

The corrosion process and the coating degradation alter the artifact surface by changing both its color and its uniformity [1]. The corrosion detection and its quantification, therefore, can be attempted either by looking at the color changes or by trying to measure the surface uniformity change [2]. One of the main problems of an image processing, which tries to measure the color change by looking at the amplitudes of the color components, is the sensitivity to the environmental conditions, i.e. to the directions of the light sources and to their chromatic composition. This approach requires observing the artifacts before the corrosion process starts, usually after restoration, in order to have a reference image. Then the artifact has to be re-analyzed to highlight color differences, but all these operations require a precise control of the lighting conditions to obtain meaningful results.

On the other hand, the surface uniformity can be assessed by looking at the local image changes that are less sensitive to the actual lighting conditions, provided that similar light sources are used to produce similar image contrasts, so that this approach might be in principle more robust for the evaluation of the surface condition.

Several approaches can be followed to obtain information about the image uniformity such as wavelet processing [3], [4], small kernel derivative operators such as Prewitt and Sobel [5], and the classical [6] and multiresolution [7] bidimensional Fourier Transform (2D-FFT). All these approaches can allow one to gain the required information if a suitable tuning of the algorithm is performed. After some preliminary tests that revealed the potential feasibility of the different approaches, the authors decided to employ the classical 2D-FFT due to its simplicity and the possibility of performing different kinds of post-processing in the frequency domain that could be used to monitor protective coatings failure and corrosion processes occurring onto the

sample surface as described in the following. The 2D-FFT algorithm maps single numbers contained inside a matrix, which represents the image pixels, into another matrix in the frequency domain. Artifact images, however, are usually taken as color pictures, so that each pixel is usually composed of a triplet (typically the red, green and blue intensities in the RGB space).

It is therefore possible to perform the 2D-FFT either on one of the colors or on a parameter derived from the colors, such as a weighted color sum, to obtain a black and white representation [8] or eventually on a parameter obtained in a different color space such as the brightness parameter of HSV (hue, saturation, and brightness) color space [9].

All the results described in the following refer to analyzes performed on the brightness value in the HSV color space, which proved to give the best results in this case, where localized corrosion phenomena occur due to the presence of defects in the protective coating which lead to a corrosion products growth proceeding over small fractions of the entire surface area, at least at the beginning. The entire process can, however, be applied to other parameters as well. As anticipated, the 2D-FFT is to be regarded as the basis of a subsequent process to extract one or more parameters capable of giving information about the surface uniformity. As an example, starting from the raw FFT, it is easy to see if the image has peaks at specific frequencies which denotes corrosion patterns often due to specific coating failures. The processing described in the following is designed to discard these kinds of information and to provide only a single number representative of the surface non-uniformity, but of course other more sophisticated processing can be performed if necessary. In order to reduce the *phase* effect, i.e. the result changes due to the actual orientation of the artifact when the image is taken, the authors decided to employ only the amplitude value. Then, since the 2D-FFT process has the property of conserving the energy, the natural approach is to group the energy as a function of the spatial frequency regardless of the angular direction and this can be obtained by summing the values at equal  $x$  and  $y$  distance from the zero frequency. If an FFT algorithm that puts the zero frequency at image center is used, this turns out in computing:

$$A_m(f)^2 = \sum_{i=-f}^f FFT(-f, i)^2 + \sum_{i=-f}^f FFT(f, i)^2 + \sum_{i=-f+1}^{f-1} FFT(i, -f)^2 + \sum_{i=-f+1}^{f-1} FFT(i, f)^2 \quad (1)$$

where  $FFT$  is the matrix containing the 2D-FFT transformed values,  $f$  is the spatial frequency which spans in the range of 0 to  $\frac{N}{2} - 1$ , and the processing simplification due to the intrinsic 2D-FFT symmetry has not been used in the equation for clarity.

For an image composed of  $N \times N$  pixels, eqn. 1 results in an  $\frac{N}{2}$  length vector, whose components are representative of the average energy amplitude at a certain spatial frequency.

At this point, to remove the effect of the actual exposure, which acts as a scaling factor for the energy, it is possible to compute an adimensional parameter  $\alpha(h)$  as the fraction of the high frequency spatial energy with respect to the total energy as:

$$\alpha(h) = 1 - \frac{\sum_{i=0}^h A_m(i)^2}{\sum_{i=0}^{\frac{N}{2}-1} A_m(i)^2} \quad (2)$$

where  $\alpha(h)$  is the energy fraction associated to frequencies greater than  $h$ , which spans in the range 0 to 1.

Eventually, a simple uniformity indicator can be used as the  $\alpha_{cut}$  value that corresponds to a predefined fraction of energy:

$$\alpha_{cut}(p) = \frac{\min(h) \vee (\alpha(h) > p)}{\frac{2N}{2} - 1} \quad (3)$$

where  $p$  is the desired energy fraction in the range of 0 to 1 and  $\alpha_{cut}$  spans in the range of 0 to 1.

In all cases, after the processing required to extract the parameter to be transformed (i.e. brightness, hue, ...) the images can be windowed to avoid border effects by applying a double raised cosine window:

$$w(x, y) = \frac{1}{4} \left[ 1 + \cos\left(\frac{x\pi}{N}\right) \right] \cdot \left[ 1 + \cos\left(\frac{y\pi}{N}\right) \right] \quad (4)$$

where  $N$  is the image dimension and  $x$  and  $y$  are the coordinates from the image center which span from 0 to  $N/2$ .

Fig. 1 shows a summary of the proposed approach applied to two simulated images: the left image resembles a uniform sample with a few spots simulating small surface damages, while the right image resembles a rough surface covered in spots, simulating a badly corroded sample. The second row in the figure shows the obtained FFT shown as black and white images. The third row shows the modulus of the FFTs as a three-dimensional plot. From these two rows it is easy to see how the damaged surface produces a wide spread FFT. The fourth row contains the result of applying eqn. 1 to compute the energy at different spatial frequencies and eventually the fifth row shows the result of applying eqn. 2. It is easy to see the large difference in the traces that reflect the amount of surface damage.

### III. EXPOSURE EFFECT AND SENSOR LINEARIZATION

The advantage of the FFT algorithm as well as of all the other cited solutions is in their intrinsic linearity so that the  $\alpha$  and  $\alpha_{cut}$ , which are computed by normalizing the values to the total energy, should be independent with respect to the image average brightness. Therefore, if both the camera sensor and the firmware inside the camera that generates the final image were linear, the results would be independent from the camera setting (shutter speed and aperture value) and from the scene illumination intensity. Unfortunately, the development firmware employed in the digital cameras is usually non-linear on purpose and applies the so called *gamma* correction in order to compress

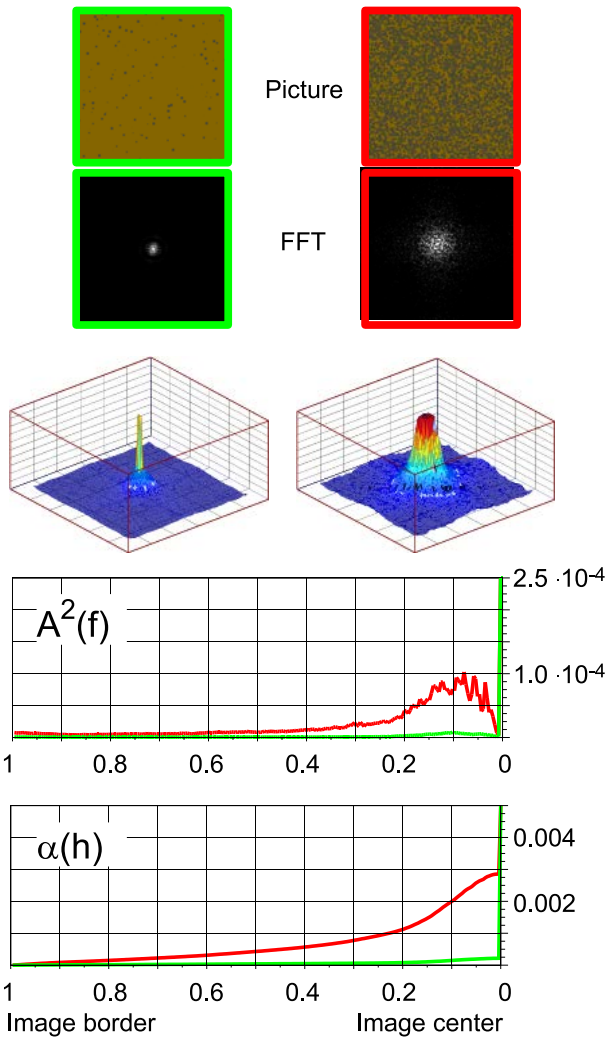


Fig. 1. Result of the proposed approach on two simulated images. From the top: the images, the resulting FFTs, the energy as a function of the spatial frequency obtained by applying eqn. 1 and the corresponding  $\alpha(h)$  obtained by applying eqn. 2. The green lines refer to the nearly undamaged surface, while the red lines refer to the damaged surface.

the tonal range and compensate for the imaging and printing system non-linearity [10]. This problem can be easily solved if the camera is capable of storing the image unprocessed i.e. in the so called RAW format, that can be developed with a software that does not apply corrections. The authors employed for the image development a widely used, open-source program referred to as *dcraw* [11] already employed in other image based researches, which is able to perform the basic development operations producing linear 16 bit per color images.

In addition to the developing problem, there is the possibility the camera sensors suffer from not negligible non-linearity since the linearity is not mandatory to obtain good images and, therefore, manufacturers may prefer to optimize other sensor parameters. To test if the problem is critical in the actual case, the authors selected two real examples of typical kinds of surfaces representing a good preserved sample and a badly corroded one and took a

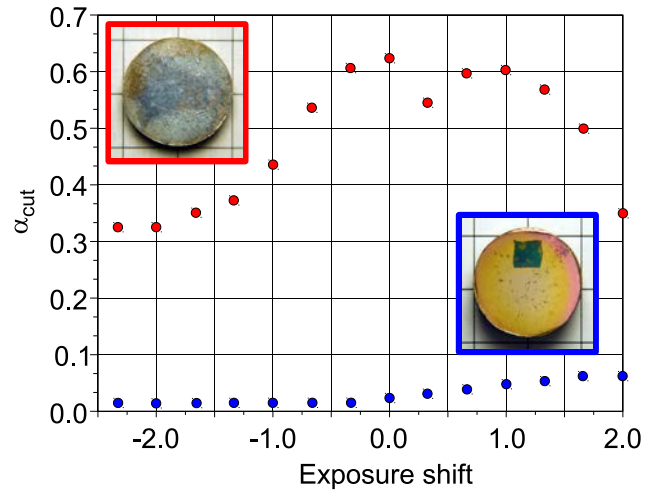


Fig. 2. The described algorithm applied to two kinds of surfaces and for different exposure values. The zero point exposure represents the exposure value suggested by the camera. It is clear how the results heavily depends on the exposure values thus suggesting the presence of a not negligible sensor non-linearity. The red dots refer to the damaged sample (top left image) while the blue ones refer to the not damaged sample (bottom right image).

series of shoots with different exposure values.

Fig. 2 shows the results obtained on images taken with a commercial camera (12Mpixels, 12 bit sensor) and with different exposure values obtained by varying the shutter speed with respect to the optimal value suggested by the camera. The usual photographic terminology is used to identify the different exposure values, which is based on the Exposure Value ( $EV$ ) defined as [12]:

$$EV = \log_2 \left( \frac{F^2}{t} \right) \quad (5)$$

where  $F$  is the relative aperture number (usually referred to as  $F$ -number) and  $t$  is the exposure time, usually referred to as *shutter time*.

In the same way the  $F$ -stop exposure change is defined as:

$$F\text{-stop} = \log_2 \left( \frac{EV_{ref}}{EV} \right) \quad (6)$$

where  $EV_{ref}$  is the exposure reference value. As an example, for fig. 2 the exposure was changed in the range of  $\pm 2F$ -stop i.e. changing the shutter time from  $1/4$  to 4 times the value suggested by the camera metering system.

It is clear how the results heavily depend on the exposure, especially in the case of the damaged sample, suggesting the presence of a not negligible sensor non-linearity.

The problem of the sensor non linearity and of its identification and correction has been widely discussed in the literature and several approaches have been proposed ([13], [14]). Basically, the identification can be performed either by taking pictures of a sample uniformly lighted and with patches having known reflectivity or by taking several pictures of the same scene with different exposures and by processing the results of the corresponding pixels. Since insuring a uniform lighting is difficult, the authors employed this last approach.

A grayscale target (fig. 3) with 15 patches having logarithmic scale reflectivity was used and a series of pictures were taken by varying the exposure time in the range of  $1/4000$  s to 1 s and with an aperture  $F = 11$ , which correspond to Exposure Values in the range of about 6 to 18. The pictures were taken with EV spaced apart of about  $1/3F$ -stop, therefore obtaining a total of 37 pictures. The images were developed by using the *dcraw* software and the average value corresponding to the 15 chart patches was computed for each picture, therefore obtaining 37 values for each patch. Fig. 3 shows the 15 lines corresponding to the brightness of each patch in the different pictures taken at different exposures.

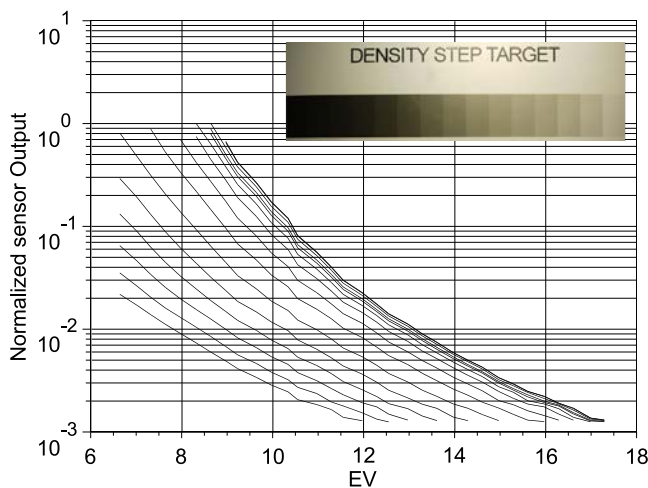


Fig. 3. The 15 traces corresponding to the average brightness computed for the 15 different patch areas vs. exposure values. In a log-log scale a linear sensor would produce a family of straight lines. The traces confirm the sensor non-linearity. On the top right a picture of the grayscale target.

Since the *EV* is proportional to the logarithm of the actual light collected by the sensor and the amplitude scale in the picture is logarithmic, the 15 traces should be straight lines if the sensor were linear, while their curvature confirms the sensor non-linearity. Since in this research the actual luminance is not required and a fast data processing is required due to the number of FFTs to be performed, it was decided to implement the correction in the form of a look-up table i.e. storing three vectors, one per color, of 4095 components each corresponding to all the possible values generated by the sensor. The identification of the look-up table coefficients was obtained by using a four-step process:

- Too low and too high acquired values were removed from the available data. This is required to remove black values stuck at the sensor noise and white saturated values at sensor limit.
- The values of each trace were interpolated determining the equivalent luminance corresponding to each possible sensor output:

$$m(j, k) < i < m(j, k + 1)$$

$$v_i(j, i) = \frac{v(k + 1) - v(k)}{m(j, k + 1) - m(j, k)} \cdot [i - m(j, k)] + v(k) \quad (7)$$

where  $m(j, k)$  are the measured value of the  $j^{\text{th}}$  patch corresponding to  $k^{\text{th}}$  exposure and  $v$  are the luminance corresponding to the different exposures.

- The traces, which had different values due to the different patch reflectance, were scaled to have the same value at a key point which was selected at the center of the pixel value distribution for a correctly exposed image (see fig. 4). This way it was possible to obtain a set of nearly superposed traces:

$$v_i(j, i) = \frac{v_i(j, i)}{v_i(j, i_k)} \quad (8)$$

where  $i_k$  is the index located at the center of the pixel distribution in the case of a correctly exposed image and  $v_i(j, i)$  is the interpolated value.

- All the available values of each pixel level (i.e. all the values which were filled by eqn. 7 during the second step) were averaged and the average was used as the value for the look-up table. The standard deviation of the different values of each pixel was below 3% of the mean value  $v_{mi}(i)$  for each point confirming the correctness of the procedure.

$$v_{mi}(i) = \frac{\sum_{j, v_i(j, i) > 0} v_i(j, i)}{\sum_{j, v_i(j, i) > 0} 1} \quad (9)$$

Fig. 4 shows the results obtained with the commercial camera used for this research. The picture shows the normalized look-up table values i.e. the equivalent camera sensor response for the three colors (red, green and blue lines) and, on the left, three examples of histograms of the pixel distribution one can obtain for three pictures taken at  $-1F$ -stop, at the correct exposure, and at  $+1F$ -stop (black lines). It is clear how the pixel distributions span over a non linear sensor response range and, therefore, how an exposure change produces a *distorted* image brightness distribution and therefore a different FFT.

Fig. 5 shows the results of using eqns. 2 and 3 after correcting the pixel values by means of the curve shown in fig. 4. Now, as expected, the exposure effect is greatly reduced and the  $\alpha_{cut}$  value reduced due to the great reduction of the luminance non linearities. This means that by using the proposed procedure a single picture of the artifact, taken by using the default camera setting, can be used for the measurements, without worrying about the slight exposure changes due to the overall lighting.

## IV. EXPERIMENTAL RESULTS

### A. Reference samples

The proposed imaging processing was tested in laboratory on several reference samples, which were prepared by coating them with different protective films, specifically

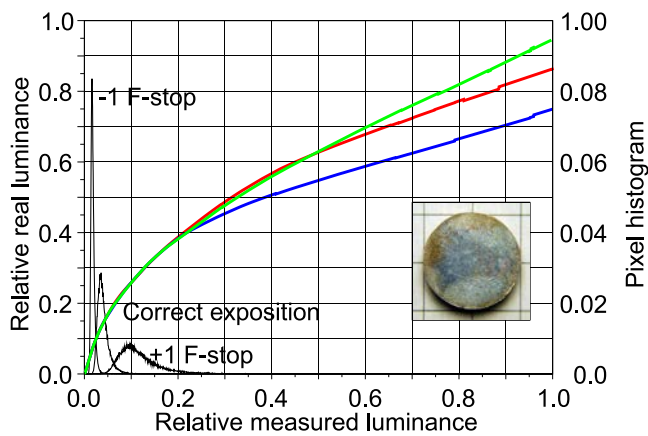


Fig. 4. Normalized sensor response for the three colors (red, green and blue lines) and an example of the pixel brightness distribution one can obtain in the case of three pictures taken with the camera suggested exposure and with  $\pm 1F$ -stop exposure values (black lines). The pixel distributions refer to the image in the rectangle.

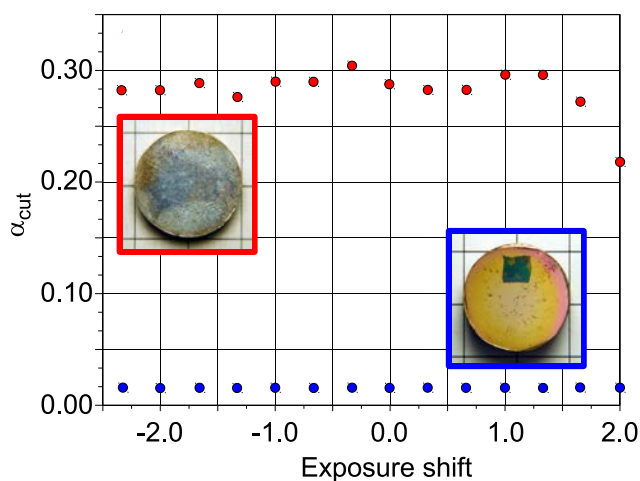


Fig. 5. Result obtained on the same images of fig. 2, but with the sensor linearization obtained by employing the curve of fig. 4. The red dots refer to the damaged sample (top left image) while the blue ones refer to the not damaged sample (bottom right image). Now the exposure effect is minimal, at least in the exposure range of  $\pm 1F$ -stop, when the entire image dynamic range is within the sensor dynamic.

selected to be suitable for the protection of metallic antiquities. The samples were prepared starting from silver-copper alloy disks (Ag90Cu10 atomic percentage - 20 mm diameter, 2 mm thickness) mirror-like polished. The protective layers were created by using a PECVD (Plasma Enhanced Chemical Vapor Deposition) reactor to deposit  $\text{SiO}_x$  thin films with thickness of about 500 nm. These films are reversible, characterized by optical transparency, high conformability to the surface morphology, high chemical stability and high barrier properties against aggressive gases. For these reasons they have already been proposed for the protection of silver artifacts from tarnishing [15]. The chemical properties of these coatings depend on the deposition conditions [16], since higher discharge input powers usually lead to better barrier properties of the deposited layer. Unfortunately, high powers are also connected to an high ion bombardment of the substrate, which

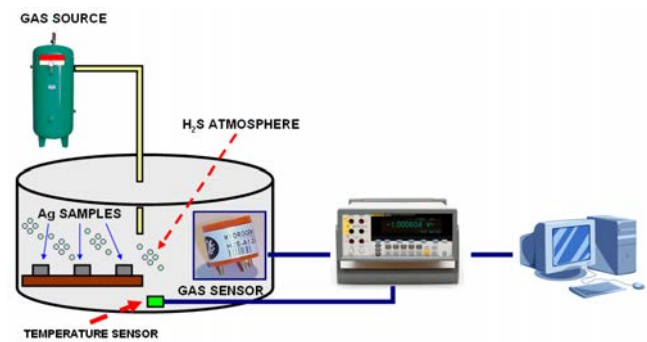


Fig. 6. Setup for the accelerated aging test. The set-up is composed of a chamber equipped with a  $\text{H}_2\text{S}$  vapors source, a commercial  $\text{H}_2\text{S}$  sensor, a temperature sensor, a multimeter and a PC.

can damage the surface; so that a compromise should be found.

The  $\text{SiO}_x$  thin films were deposited by using a plasma fed with 1 sccm (standard cubic centimeters per minute) of tetraethoxysilane (TEOS), 10 sccm of oxygen and 29 sccm of argon. Four different discharge powers were used for deposition: 50 W, 100 W, 200 W and 250 W. Some samples were also left uncoated for comparison.

After the plasma deposition, small Ag pads were sputtered on some of the disks to allow for impedance measurements [17]. Such impedance measurements can be used to assess the insulating nature of the deposited coating, which can lead to high protective effectiveness against corrosion. This is in fact a powerful method for estimating the protective capability for highly insulating materials, such as the  $\text{SiO}_x$  film deposited at high input power, but cannot be easily employed with the coatings deposited at low power that appear as poor electrical insulators. The pads appear as small bright squares in the images, the image areas interested by such pads were excluded by all subsequent image analyzes.

An accelerated ageing test was then performed both on the bare and on the coated samples by using the setup shown in fig. 6. The samples were inserted into a reaction chamber maintained at  $20^\circ\text{C} \pm 2^\circ\text{C}$  and a single injection per day of hydrogen sulfide ( $\text{H}_2\text{S}$ ) capable of producing a gas concentration of about 1 ppm, was performed. The  $\text{H}_2\text{S}$  concentration in the chamber was measured by means of an electrochemical commercial sensor, the ageing lasted for a total of 35 days.

### B. Imaging setup

In order to perform a comparison between different frequency based image transformations it is obviously required to know the spatial resolution of the compared FFTs, and this in turns requires to know the shooting conditions (i.e. lens focal, shooting distance and image sensor size). If the same camera and lens are used, the only relevant parameter becomes the shooting distance, so that insuring different images of the same artifact are comparable only requires keeping the camera distance fixed. Of course, to perform a successful comparison, it is required that the



image is correctly focused and this in turn requires that the surface to be analyzed be flat and orthogonal to the camera within the camera depth of field. This might be in general a problem, since the artifacts are usually three dimensional objects, but the problem can be reduced by selecting small areas to capture, with the additional advantage of having a higher spatial resolution. On the other hand, a too high resolution could lead to miss some features due to the reduced capture area unless a large amount of pixels is used that would slow down the processing, thus a compromise is required.

The authors eventually decided to employ a spatial resolution of about  $15 \mu\text{m}$ , a value which can be easily obtained with lenses having focal in the range of 50 mm to 100 mm (equivalent to the 35 mm camera format) and with shooting distances in the range of 10 cm to 20 cm. This way it is possible to perform FFTs with dimensions  $256 \times 256$  pixels corresponding to image areas of about  $4 \text{ mm} \times 4 \text{ mm}$ .

### C. Obtained results

In order to test the proposed algorithm effectiveness the following procedure was used:

- A square area was selected on each sample excluding the pad-covered area when present. Areas with dimensions in the range of  $512 \times 512$  to  $896 \times 896$  pixels were obtained in this way. This is equivalent to areas in the range of about 7.5 mm to 13 mm, which are values large enough to be sure to catch and average the different conditions of the sample surfaces.
- A series of  $256 \times 256$  points 2D-FFT were computed each time shifting the FFT area by 128 pixels in both the  $x$  and  $y$  directions obtaining, therefore, 9 to 36 different estimations. The FFTs were performed on the brightness value computed according to the HSV paradigm [9] after some preliminary tests showed the good performance of this index.
- The  $\alpha_{cut}(0.006)$  was computed for each FFT thus obtaining 9 to 36 values for each sample. Mean and standard deviation were computed for each set to test the procedure stability for different portions of the same image.

Fig. 7 summarizes the obtained results. In the middle the pictures of the five samples taken after the ageing times shown on the left. In the upper part the results obtained with the proposed solution, while at bottom, for comparison, the results one could obtain by computing the average hue of the analyzed areas. Each bar height represents the standard deviation of the means obtained on each area. It is clear how the hue based method is not able to detect the corrosion presence especially in the initial phase, while the frequency based approach appears highly sensitive to the protective coating failure.

At a visual observation a diffuse tarnishing is observed onto the uncoated sample. The FFT response is, however, quite similar to the one obtained for the samples coated with  $\text{SiO}_x$  film deposited at high input power and on which no surface tarnishing evidences can be detected. Higher values were obtained, on the contrary, for samples coated

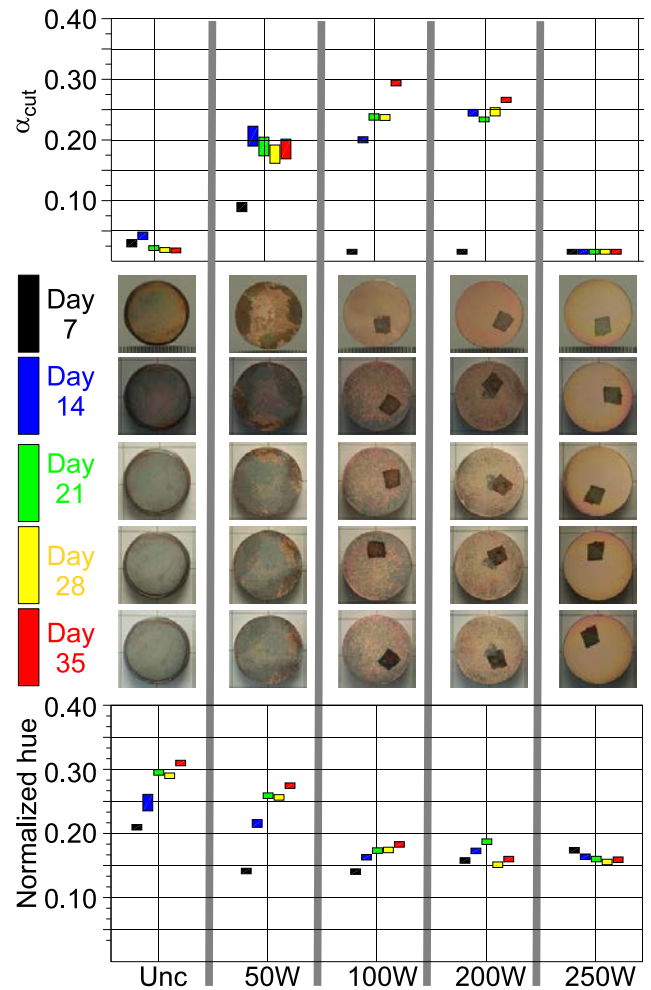


Fig. 7. Examples of results obtained by the proposed method on an uncoated silver sample and on four samples coated with  $\text{SiO}_x$  films deposited at different input powers (in the range of 50 W to 250 W) and exposed to the aggressive atmosphere for different periods (from 7 to 35 days). Each bar height shows the standard deviation of the mean  $\alpha_{cut}$  computed on the available area for the analysis. For comparison, at figure bottom, the result one could obtain by using an amplitude-based measurement based on the average image hue in the HSV color space. It is clear how the hue based method is not able to detect the corrosion presence in the initial phase.

with  $\text{SiO}_x$  film deposited at low input power, which showed a less protective effectiveness and on which noticeable localized tarnishing attacks are consequently observed. As a matter of facts,  $\text{SiO}_x$  thin film deposited at 250 W shows high barrier properties against the aggressive vapors. Consequently, no significant changes in surface uniformity can be detected as a function of the exposure time, that turns out in a uniform surface. The same way, no changes in surface uniformity are observed onto the uncoated surface, on which the tarnishing film grows in an homogeneous way. On the contrary, the FFT response obtained on samples coated with  $\text{SiO}_x$  thin films deposited at lower input powers is quite different. In facts, on these samples the presence of localized corrosion attacks can be observed, which led to uniformity changes and, consequently, to high  $\alpha_{cut}$  values.

It is therefore possible to conclude that, notwithstanding the proposed algorithm is not able to give quantitative information about the coating failure and the corrosion mechanism, the obtained results are able to underline the presence of dangerous situations for the artefact and to highlight when immediate restoration is required to avoid further damages.

## V. CONCLUSIONS

This paper describes a simple imaging approach that can be used as a cheap alternative to conventional invasive techniques such as EIS and optical and electron microscopy to ensure a long and stable life to cultural property, not only made of metals, to identify the conservation problems and to guarantee their safe exposure. The approach does not require either moving the artifacts to a laboratory or using special precautions for the lighting conditions; so that it can be used in museums without affecting its usability. The processing is based on the use of RAW images, on a linear development process and on a procedure to correct the sensor non-linearity and allows one to successfully apply the procedure even though the exposure changes from one shoot to another up to  $\pm 1F$ -stop, thus really lessening the lighting constraints. The described solution relies on a frequency domain analysis based on a 2D-FFT transform, but other frequency-sensitive approaches based, as an example, on wavelet transformation and small kernel filters can be used as well on the images generated with the described linearization process.

Although the described technique, which is based mainly on the measurements of the surface uniformity changes, does not allow a quantitative assessment of the corrosion rate, it has proved to be an effective approach to assess the stability of protective coatings, as well as an easy and fast method for the estimation of the aggressiveness of the environment in which the artifacts are exposed.

The proposed approach, that can be used also by non trained operators can, therefore, be a preventive routine measurement that should help conservators deciding when more invasive restoration/conservation procedures are required.

## REFERENCES

- [1] M. Thornbush and H. Viles - "Integrated digital photography and image processing for the quantification of colouration on soiled limestone surfaces in Oxford, England", *Journal of Cultural Heritage*, Vol. 5, pp. 285-290, 2004
- [2] E. Angelini, S. Corbellini, F. Ferraris, S. Grassini, A. Neri, M. Parvis, M. Piantanida - "FFT-based imaging processing for cultural heritage monitoring", in *Proc. I2MTC 2010, IEEE Int. Instrum. Meas. Technol. Conf.*, Austin TX, pp. 1106-1111, 2010
- [3] M. Antonini, M. Barlaud, P. Mathieu, I. Daubechies - "Image coding using wavelet transform" *IEEE Transactions on Image Processing*, Vol. 1, No 2, pp. 205-220, 1992
- [4] D.M. Chandler, S.S. Hemami - "Dynamic contrast-based quantization for lossy wavelet image compression", *IEEE Transactions on Image Processing*, Vol. 14, No 4, pp. 397-410, 2005
- [5] H.G. Senel - "Gradient Estimation Using Wide Support Operators", *IEEE Transactions on Image Processing*, Vol. 18, No. 4, pp. 867-878, 2009
- [6] R.W. Cox, Tong Raoqiong - "Two- and three-dimensional image rotation using the FFT", *IEEE Transactions on Image Processing*, Vol. 8, No. 9, pp. 1297-1299, 1999

- [7] R. Wilson, A.D. Calway, E.R.S. Pearson - "A generalized wavelet transform for Fourier analysis: the multiresolution Fourier transform and its application to image and audio signal analysis" *IEEE Transactions on Information Theory*, Vol. 38, No. 2 part 2, pp. 674-690, 1992
- [8] CIE Publication No.18.2, - "The Basis of Physical Photometry", 1983
- [9] R.C. Gonzales, R.E. Woods - "Digital Image Processing", Prentice Hall, 2007
- [10] M. Stokes, M. Anderson, S. Chandrasekar, R. Motta - "A Standard Default Color Space for the Internet - sRGB", ver. 1.10, 1996, available at <http://www.w3.org/Graphics/Color/sRGB.html>
- [11] C. Manders, S. Mann - "True images: a calibration technique to reproduce images as recorded", in *Proc. of the Eighth IEEE International Symposium on Multimedia (ISM'06)*, 2006
- [12] S.F. Ray - "Camera Exposure Determination" in: *The Manual of Photography: Photographic and Digital Imaging*, 9th ed. Oxford: Focal Press.
- [13] M.D. Grossberg, S.K. Nayar - "What is the Space of Camera Response Functions?", *Proceedings of the 2003 IEEE Computer Society Conference on Computer Vision and Pattern Recognition (CVPR03)*, 2003
- [14] M.D. Grossberg, S.K. Nayar - "Determining the Camera Response from Images: What Is Knowable?", *IEEE Transaction on pattern analysis and machine intelligence*, Vol. 25, No. 11, pp. 1455-1467, 2003
- [15] E. Angelini, R. d'Agostino, F. Fracassi, S. Grassini, F. Rosalbino, - "Surface Analysis of PECVD Organosilicon Films for Corrosion Protection of Steel Substrates", *Surface and Interface Analysis*, Vol. 34, pp. 155-159, 2002
- [16] E. Angelini, S. Grassini, D. Mombello, A. Neri, M. Parvis - "An imaging approach for a contactless monitoring of the conservation state of metallic works of art" *Applied Physics. A, Material science & processing*, Vol. 339, 2010
- [17] A. Carullo, S. Grassini, M. Parvis - "Measurement Procedures for the Electrical Characterization of Oxide Thin Films", *IEEE Transactions on Instrumentation and Measurement*, Vol. 58, No. 5, pp. 1398-1404, 2009



**Emma Angelini** born in Torino in 1951, was graduated in Chemistry at Torino University. She is in Politecnico di Torino since 1976 and is now Full Professor of Applied Physical Chemistry in the Faculty of Engineering, Information Sector. Her research areas are: Corrosion and protection of metallic materials, as stainless steels, amorphous and nanocrystalline alloys, biomaterials for dentistry, tangible Cultural Heritage; plasma chemistry and coatings deposition. She is involved in National and European projects on corrosion and protection of metals and is member of the European Federation of Corrosion (EFC).



**Simone Corbellini** was born in Italy in 1977. He received the M.S. degree in Electronic Engineering in 2002 from Politecnico di Torino, Italy, and the Ph.D. degree in metrology in 2006 from Politecnico di Torino, Italy. His main fields of interest are digital signal processing, distributed measurement systems, and intelligent microcontroller-based instrumentation. At present, he is working on the development of networks of low-power wireless sensors for environmental, biomedical and chemical quantities.





**Franco Ferraris** was born in Italy in 1945. He received the degree in Electrical Engineering from Politecnico di Torino in 1969. In 1990 he became full professor of Electronic Measurements at University of Catania, Italy. Since 1991 he is with the Dipartimento di Elettronica of the Politecnico di Torino. He is past head of this department. His fields of interest include automatic controls and system theory, biomedical measurements, intelligent measurement systems and intelligent sensors.



**Sabrina Grassini** was born in Italy in 1972. She received the M.S. degree in Chemistry in 1999 from Università di Torino, Italy, and the Ph.D. degree in metallurgical engineering in 2004 from Politecnico di Torino, Italy. Currently she is an assistant professor in Chemistry with the Dipartimento di Scienza dei Materiali e Ingegneria Chimica, Politecnico di Torino. Her researcher areas include plasma chemistry and coating deposition, corrosion and protection of metallic materials, and conservation of

cultural heritage.



**Alessandra Neri** was born in Italy, in 1982. She received the M.S. degree in electronic engineering and the Ph.D. degree in metrology from Politecnico di Torino, Torino, Italy, in September 2006 and December 2009, respectively. She is currently a Research Assistant with the Department of Electronics, Politecnico di Torino. Her main fields of interest are the development and the metrological characterization of acquisition systems and sensors for physical and chemical quantities.



**Marco Parvis** was born in Italy in 1958. He received his MS degree in electrical engineering in 1982 from the Politecnico di Torino, Italy, and a Ph.D. degree in Metrology in 1987. He is now full professor of Electronic Measurements at Politecnico di Torino. He is Past Dean of the Second Faculty of Engineering of Politecnico di Torino and Fellow Member and chair of the TC 25 Medical Measurement of the IEEE Society on Instrumentation and Measurement. His main fields of interest are: intelligent instru-

mentation, application of signal processing to measurement, biomedical and chemical measurements. He is author of more than one hundred publications.